Electronic Supplementary Information

for

N-acetylglucosamine-based efficient phase-selective organogelators for oil spill remediation

Somnath Mukherjee, Congdi Shang, Xiangli Chen, Xingmao Chang, Kaiqiang Liu, Chunmeng Yu and Yu Fang*

Key Laboratory of Applied Surface and Colloid Chemistry, Ministry of Education, School of Chemistry and Chemical Engineering, Shaanxi Normal University, Xi'an 710062, P. R. China.

*Email: yfang@snnu.edu.cn

1. Materials and methods:

All reagents and liquids were dried prior to use according to standard methods. All the reagents were purchased from commercial suppliers. Commercial reagents were used without further purification unless otherwise stated. All reactions were monitored by Thin Layer Chromatography (TLC) on Silica gel 60-F_{254} and chromatograms were visualized under UV light and by charring following immersion in a 10% ethanolic solution of sulfuric acid. Flash chromatography was performed with Silica Gel 230-400 mesh. NMR spectra were measured using BRUKER AVANCE 400 NMR spectrometer. Melting points were recorded on a Stuart, SMP-30 melting point apparatus. Elemental analyses were performed using PerkinElmer 2400 CHN elemental analyzer using acetanilide as a calibration standard. Fluorescence measurements were performed at room temperature on a time-correlated single photon counting fluorescence spectrometer (Edinburgh Instruments FLS 920).

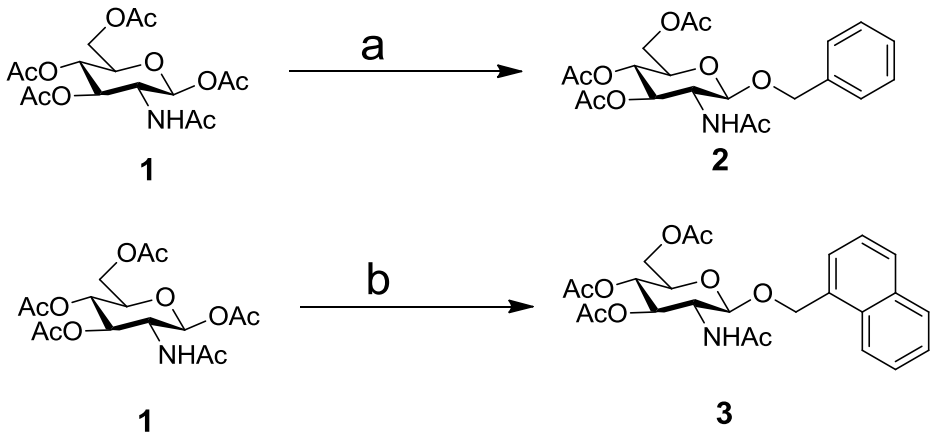

Scheme S1: Synthesis of the amphiphile **2** and **3**.

Reagents and conditions: (a) BnOH, H_2SO_4-Silica, Microwave, 110 ℃, 30 min, 82%. (b) 1-Napthalenemethanol, H_2SO_4-Silica, Microwave, 110 ℃, 40 min, 92%.

2. Synthesis and characterization of benzyl 2-Acetamido-3,4,6-tri-*O*-acetyl-2-deoxy-β-D-glucopyranoside (2):

A solution of per-*O*-acetylated *N*-acetyl glucosamine (**1**, 2 g, 5 mmol), benzyl alcohol (0.359 mL, 3.33 mmol), and H_2SO_4-silica (10 mg) in dry DCE (7 mL) was stirred in a 10 mL microwave vial using a Biotage Initiator 1 microwave reactor at 110 ℃ for 30 min. The reaction was followed by TLC. After the completion of the reaction (30 min), reaction mixture was filtered through Celite and washed with CH_2Cl_2 ensuring complete recovery. Then, the reaction mixture was washed successively with sat. $NaHCO_3$ (2 × 10 mL) and brine (10 mL). The mixture was concentrated in vacuo and the residue was purified by flash chromatography using *n*-hexane-EtOAc (1.5:1) to afford pure compound (1.83 g, 82 %). M.P. 165 ℃, ^{1}H NMR ($CDCl_3$, 400 MHz) δ: 7.29-7.37 (m, 5H), 5.32 (d, J = 8 Hz, 1H), 5.20 (t, $J_1 = J_2 = 12$ Hz, 1 H), 5.09 (t, $J_1 = 12$ HZ, $J_2 = 8$ Hz, 1 H), 4.90 (d, J= 16 Hz, 1H), 4.62 (t, $J_1 = 8$ HZ, $J_2 = 12$ Hz, 2 H), 4.28 (dd, $J_1 = J_2 = 4$ Hz, 1 H), 4.17 (dd, $J_1 = J_2 = 4$ Hz, 1 H), 3.97 (q, J = 4 Hz, 1H), 3.67 (m, 1H), 2.11 (s, 3H), 2.01 (s, 3H), 2.00 (s, 3H),1.91 (s, 3H) ^{13}C NMR (100 MHz, $CDCl_3$) δ: ppm 170.96, 170.73, 170.17, 169.38, 136.94, 128.49, 128.07, 99.49, 72.48, 71.78, 70.67, 68.70, 62.19, 54.52, 23.27, 20.76, 20.68, 20.62MS (ESI): m/z calcd for [M + Na^+], 460.1584; found, 460.1572 m/z calcd for [M + K^+], 476.1323; found, 476.1312 Anal Calcd for $C_{21}H_{27}NO_9$ C 57.66 H 6.22 N 3.20 found**.** C 57.70 H 6.10 N 3.09. Spectral data is in accordance with previously reported values.[1]

3. Synthesis and characterization of 1-Napthyl 2-Acetamido-3,4,6-tri-*O*-acetyl-2-deoxy-β-D-glucopyranoside (3):

A solution of per-*O*-acetylated *N*-acetyl glucosamine (**1,** 2 g, 5 mmol), 1-napthalenemethanol (0.527 g, 3.33 mmol), and H_2SO_4–silica (10 mg) in dry DCE (7 mL) was stirred in a 10 mL microwave vial using a Biotage Initiator 1 microwave reactor at 110 ℃ for 40 min. The reaction was followed by TLC. After the completion of the reaction (40 min), reaction mixture was filtered through Celite and washed with CH_2Cl_2 ensuring complete recovery. Then, the reaction mixture was washed successively with sat. $NaHCO_3$ (2 × 10 mL) and brine (10 mL). The mixture was concentrated in vacuo and the residue was purified by flash chromatography using *n*-hexane-EtOAc (1.5:1) to afford pure compound (2.30 g, 92 %). M.P 173 ℃, ^{1}H NMR ($CDCl_3$, 400 MHz) δ: 8.12-7.43 (m, 7H), 5.40 (d, J = 12 Hz, 1H), 5.07 (m, 2H), 4.97 (m, 2H), 4.52 (d, J = 12 Hz, 1H), 4.3 (dd, $J_1 = J_2 = 4$ Hz,, 1H), 4.21 (dd, $J_1 = J_2 = 4$ Hz, 1H), 3.97 (q, J = 8 Hz, 1H), 3.62 (m, 1H), 2.14 (s, 3H), 2.02 (s, 6H), ,1.97 (s, 3H), 1.63 (s, 3H) ^{13}C NMR (100

MHz, $CDCl_3$) δ: ppm 170.87, 170.74, 170.04, 169.35, 133.93, 131.90, 131.87, 129.49, 128.68, 127.86, 126.42, 126.03, 125.11, 124.33, 98.31, 72.51, 71.91, 69.00, 68.64, 62.19,54.32, 23.04, 20.80, 20.62, 20.60 MS (ESI): m/z calcd for [M + Na^+], 510.1740; found, 510.1742 m/z calcd for [M + K^+], 526.1479; found, 526.1481 Anal Calcd for $C_{25}H_{29}NO_9$ C 61.59 H 6.00 N 2.87 found**.** C 61.58 H 5.89.00 N 2.75

4. Gelation test:

A known weight (0.025 g) of the gelator and measured amount of pure liquid were taken in test tube with internal diameter (i.d.) of 10 mm and heated slowly to dissolve the gelator completely. Then the system was allowed to come to room temperature and finally the test tube was inversed. A system was regarded as gel if it is stable to inversion of the test tube.

5. Determination of Critical Gelation Concentrations (CGCs):

At first a gelation test was carried out for 35 mg of the compound in 1 mL of liquids in a test tube. If gelation test result comes positive, then the system was diluted by small measured volume of that liquid and gelation test was done again. Such type of dilution and gelation test was repeated until the gel falls apart during inversion in the test tube. Thus, the maximum amount of liquids that can be entrapped by 35 mg of the gelator was recorded and from that CGC was calculated as wt%.

6. Determination of gel-sol transition temperatures (T_{gel}):

Firstly, gels of compound **2** or **3** in toluene with different concentrations was prepared in a test tube (i.d. = 10 mm). A glass ball (230 mg, 3 mm diameter) was placed on top of the gel sample and the test tube was sealed. Then the test tube was heated in a thermo-stated oil bath and temperature was increased at a rate of 0.2 ℃ /min by temperature controller. The temperature at which the ball falls into the bottom of the gel is considered as the T_{gel} of the system. As expected, T_{gel} increased in an approximately linear way as the concentration of the gelator was increased, showing the enhancement in gel stability at high concentrations.

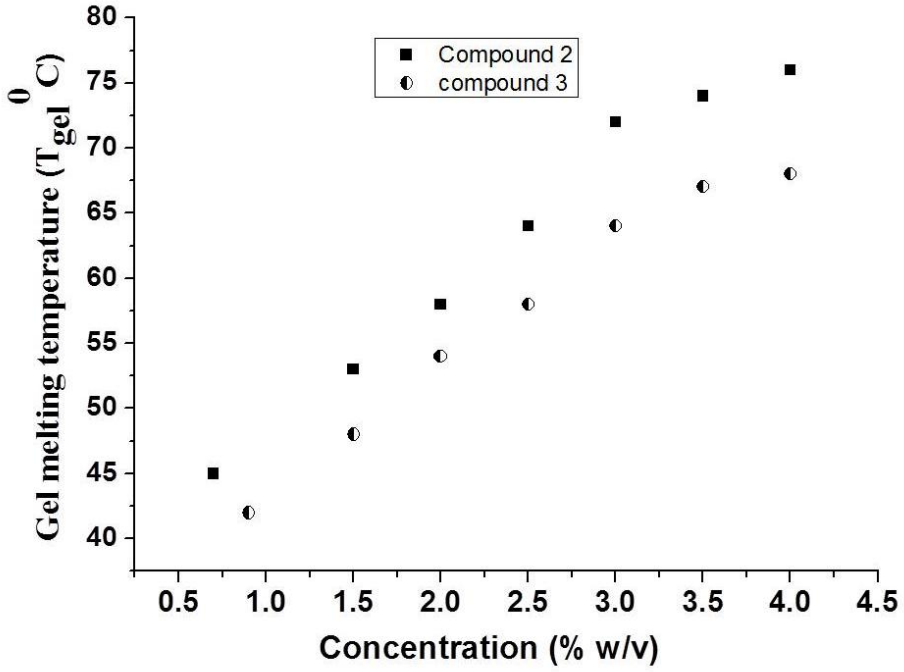

Figure S1: Plot of gel-sol transition temperature (T_{gel}) against gelator concentration of toluene gel of compound **2** and **3**.

Table S1: **Gelation abilities of compound 2 and 3 in various liquids** [a]

Liquids	**2**	**3**	Liquids	**2**	**3**
	CGC (%, w/v)	CGC (%, w/v)		CGC (%, w/v)	CGC (%, w/v)
Toluene	0.7 (TG)	0.8 (TG)	Ethanol	PS	PS
Benzene	2 (TG)	2.2 (TG)	Isopropyl alcohol	2.3 (OG)	3.5 (OG)
p-xylene	0.8 (TG)	1.2 (OG)	1-Butanol	3.5 (OG)	2 (OG)
Mesitylene	1.2 (OG)	1 (TG)	Hexanol	2.2 (OG)	2 (OG)
Hexadecane	0.9 (TG)	1.5 (TG)	Cyclohexanol	1 (OG)	3.3 (OG)
Sunflower oil	1.5 (TG)	1.1 (TG)	Octanol	1.3 (OG)	2 (OG)
Diesel	0.23 (OG)	2.2 (OG)	Water	I	I
Kerosene	0.9 (OG)	1.3 (OG)	Tetrahydrofuran	S	S
Pump oil	2.6 (TG)	3.0 (TG)	DMSO	S	S
Petrol	0.8 (TG)	0.35 (OG)	Methanol	P	P
Silicon oil	1.4 (TG)	1.8 (OG)	CH_2Cl_2	S	S
Coconut oil	1.0 (TG)	2.1 (OG)	Acetone	S	S

[a]Nature of the gels is in the parenthesis: TG = transparent gel, OG = opaque gel, S = soluble, P = precipitate, I = insoluble, PS = partially soluble

7. Proof of hydrogen bonding network:

(A) FT-IR spectroscopy studies: All FT-IR measurements were carried out on a Brucher Equinx 55 spectrometer in transmittance mode. The solution state spectra were obtained by placing the solution of gelator in dichloromethane in NaCl cells and FTIR of the xerogel was recorded by making a KBr pellet. Among several types of non-covalent interactions, hydrogen bonding is a generally encountered driving force for the formation of a supramolecular structures of LMMGs.[2] The FTIR spectroscopy measurement is very helpful in the detection and characterization of hydrogen bonding in the self-assembly of gelators. FTIR studies of both the gelators in solution state as well as gel state have been carried out to examine whether hydrogen bonding plays a role for the self-aggregation in the gel state. The FTIR spectrum of compound **2** and **3** in solution state showed NH stretching bands at 3446 cm^{-1} and 3464 cm^{-1} respectively, which are the characteristic of non-hydrogen bonded stretching frequencies. On the other hand, NH stretching band in their gel state have shifted to 3337 cm^{-1} and 3308 cm^{-1},

respectively, which are the characteristic of NH hydrogen bonded stretching frequencies. These data indicate the strong involvement of NH proton in hydrogen bonding in their supramolecular assembly and thus in gelation.

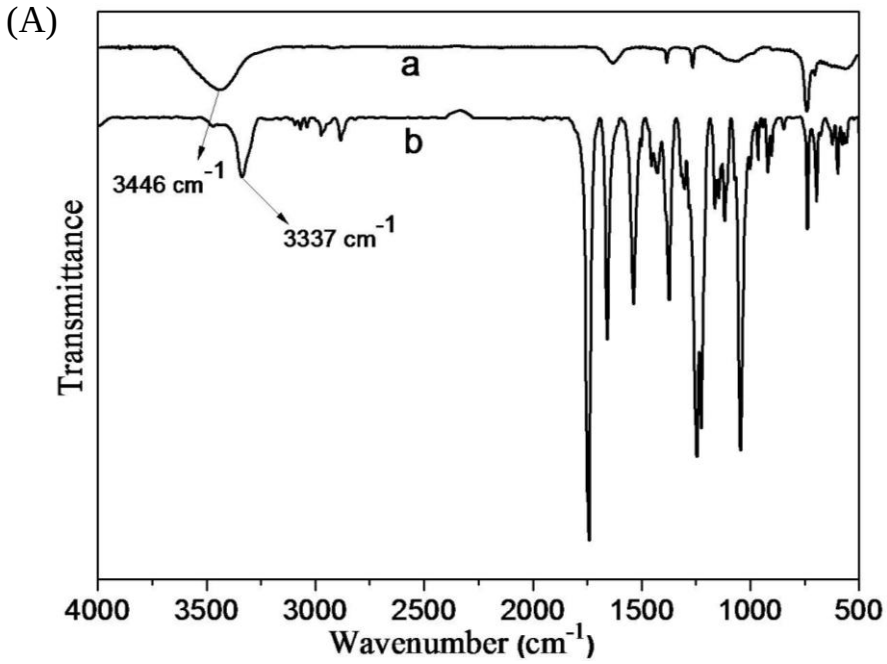

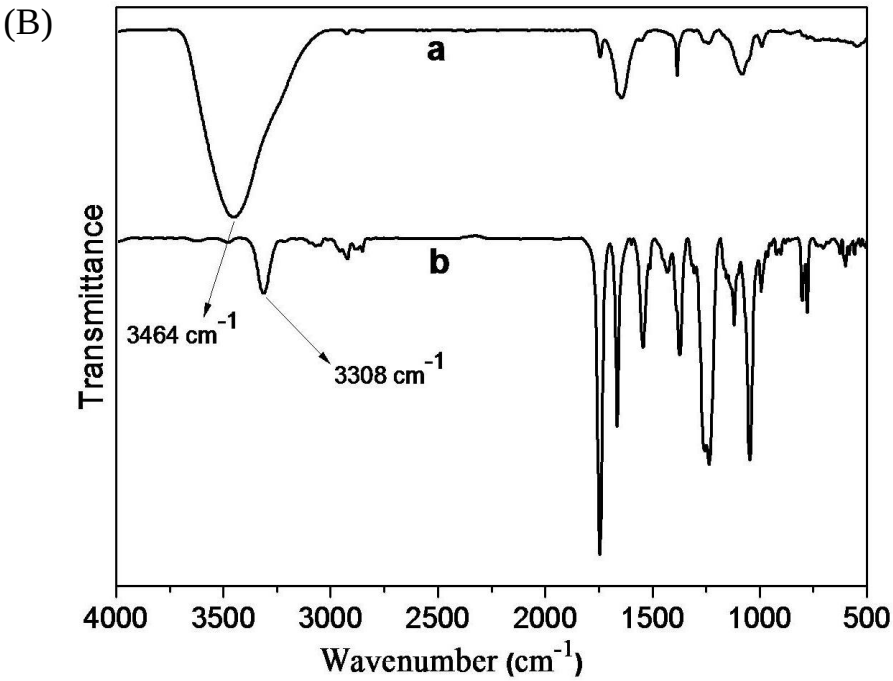

Figure S2: (A) FTIR spectra of compound **2**: (a) in CH_2Cl_2, (b) xerogel from toluene (0.7 %, w/v). (B) FT-IR spectra of compound **3**: (a) in CH_2Cl_2, (b) xerogel from toluene (0.8 %, w/v).

(B) Concentration dependent proton NMR studies: ^{1}H NMR spectroscopy is another powerful technique to study the hydrogen-bonding interaction in the gel state. Concentration-dependent ^{1}H NMR measurements for the both compound **2** and **3** were performed to inspect whether hydrogen bonding guided self-assembly is occurring in gel state. The measurement was carried out at different concentrations till its saturation (gelation) point and the results are shown bellow. Here, all NH signals are marked by alphabet **a**. Fig. S3 (A) shows that the signal of NH proton of gelator **2** appeared at 4.56 ppm at 0.08 % (w/v), but gradually it shifted to 4.95 ppm at a near gel concentration of 0.6% (w/v). Similarly, Fig S3 (B) exhibits that signal of NH proton of gelator **3** appeared at 4.20 ppm at 0.08 % (w/v), but increasingly it shifted to 4.58 ppm at a concentration of 0.7 % (w/v). Thus, for both the gelator, the consistent and significant downfield shift of the NH proton signals with increase in the gelator concentration provides another evidence for the formation of strong hydrogen bonding in the self-assembly of the gel state.

(A)

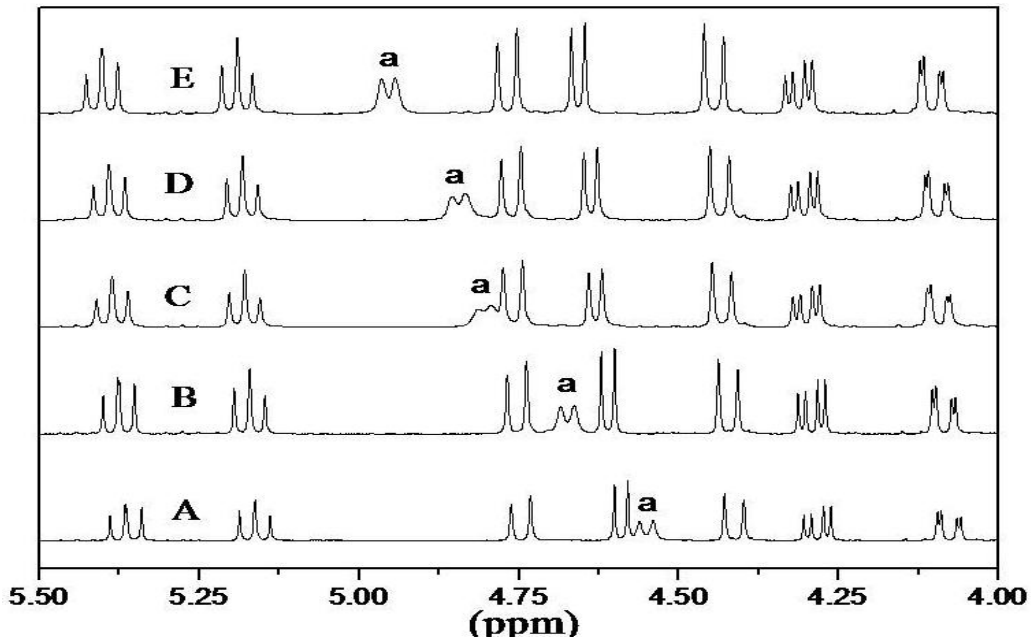

(B)

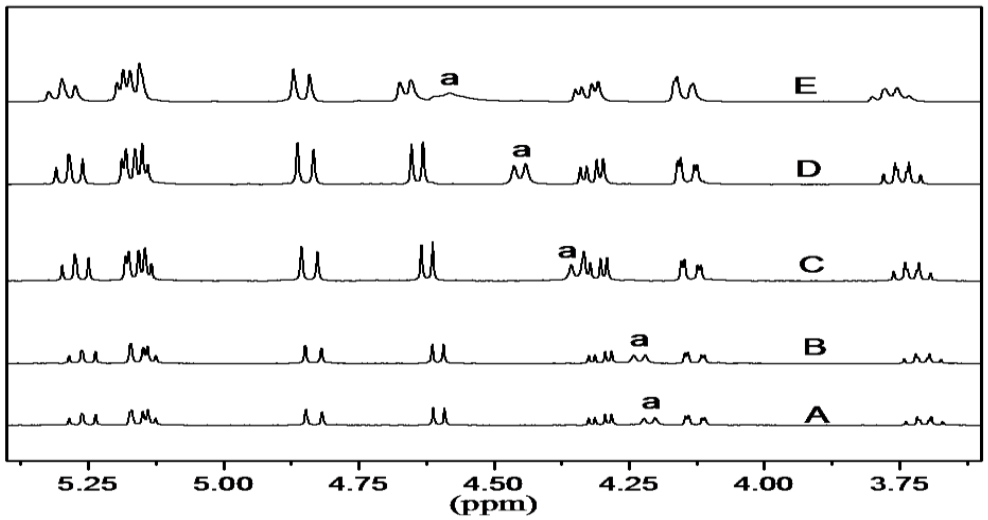

Figure S3: (A) ^{1}H NMR of the gelator **2** with increasing concentration (%, w/v). (A) 0.08%, (B) 0.2%, (C) 0.4%, (D) 0.5%, (E) 0.6% in toluene-d8 (B) ^{1}H NMR of the gelator **3** with increasing concentration (%, w/v) (A) 0.08%, (B) 0.2%, (C) 0.4%, (D) 0.5%, (E) 0.7% in toluene-d8.

8. Fluorescence measurements: Fluorescence measurements were employed for studying if there is any π-π stacking in the gel systems under study. To conduct the test, compound **3**/toluene was chosen as an example gel system. Specifically, solutions with concentrations of 0.6, 0.4, and 0.2% (w/v) were prepared by dissolving suitable amounts of the compound in certain volumes of the solvent under heating. Other solutions of smaller concentrations were obtained by diluting. The results from fluorescence measurements of the solutions are shown in Figure S4.

It is to be noted that UV-Vis measurements are not suitable for the test. This is because compound **2** is UV-Vis absorption inactive within the wavelength range studied. For compound **3**, although it is UV-Vis active, valuable UV-Vis data also cannot be obtained due to mismatching between the UV-Vis measurable concentration and the effective aggregation concentration. For example, the A value of a solution of 0.03% (w/v) of **3**, which is a concentration much lower than the CGC (0.9%, w/v) of the system, is much larger than 10, a meaningless value for UV-Vis measurements. Furthermore, fluorescence measurements for 2 cannot be conducted for the reason due to its fluorescence inactivity. Anyway, information obtained via fluorescence measurements of the solutions of compound **3** revealed the importance of π-π stacking upon the gelation of the system.

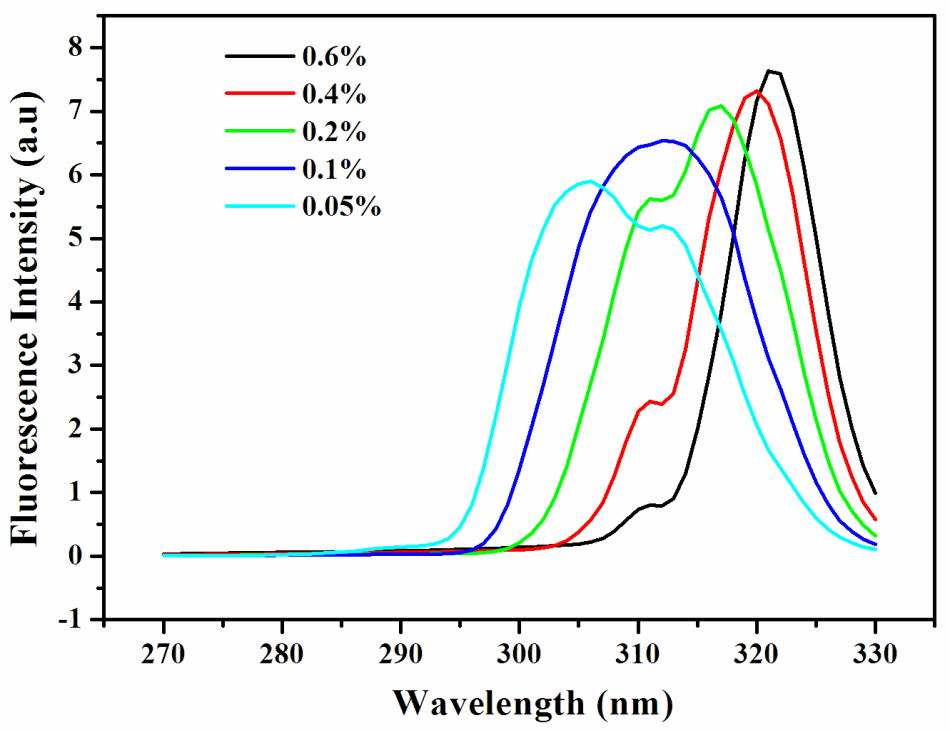

Figure S4: The excitation spectra of compound **3** in toluene recorded at different concentrations (w/v) at room temperature, λ_{em}=350 nm.

9. Rheological measurements:

Rheological measurements were performed with a stress-controlled rheometer (TA instrument AR-G2) equipped with steel coated parallel-plate geometry (40 mm diameter). The gap distance was fixed at 500 mm and a solvent-trapping device was placed above the plate to prevent solvent evaporation. All measurements were done at 25 ℃ and the gel sample on the plate was allowed to equilibrate for 10 minutes before starting the experiment. Firstly, a stress sweep at fixed frequency (1 Hz) was performed to determine the linear regime of the sample and in this study, the storage modulus G' and the loss modulus G" were measured as a function of the stress amplitude. Stress sweep shows the flowing tendency of material under stress. In that experiment G' and G" were varied with shear stress keeping frequency constant. Secondly, a frequency sweep experiment was carried out from 0.62 to 628.3 rad s^{-1} at a constant stress of 4000.0 Pa, fit within the linear visco-elastic region (LVER).

10. Microscopy studies:

A Scanning Electron Microscope (Quanta 200) operating at 5-20 kv accelerating voltage and 10 mA emission current was used to get the micrographs. In order to prepare xerogel for SEM measurement a small piece of gel was placed on a cover-slip and first dried in air and then dried for few hours under vacuum. Before imaging, the xerogel was fixed on a copper holder by using conductive adhesive tape and then coated with a thin layer of gold for 80 s at 20 kv voltages and 10 mA current using a SCD 005 cool sputter coater (Bal-Tec). AFM studies were conducted on a SOLVER P47 PRO system. A small amount of organogel sample was placed on a freshly cleaved, mica surface. Firstly, this material was dried in air by slow evaporation and then under vacuum for few hours at room temperature. Finally the images were taken using SOLVER P47 PRO atomic force microscope.

In the quest to obtain a visual insight into the morphological features of these organogels, the supramolecular 3D network was inspected by scanning electron microscopy (SEM) and atomic force microscopy (AFM) studies. The gelator **2** showed the different types of fibrous network in its gels with toluene, benzene and with a cyclohexane at their cgc. Gelator **3** also exhibited cross linked fibrous type of morphologies in its toluene and *p*-xylene gel state but the nature and diameter of the fibers were found to be different for both the solvents. The fibrous morphology of the toluene gels for both the gelator was additionally confirmed by atomic force microscopy (AFM) and the AFM images supported the similar kind of entangled fibril structure.

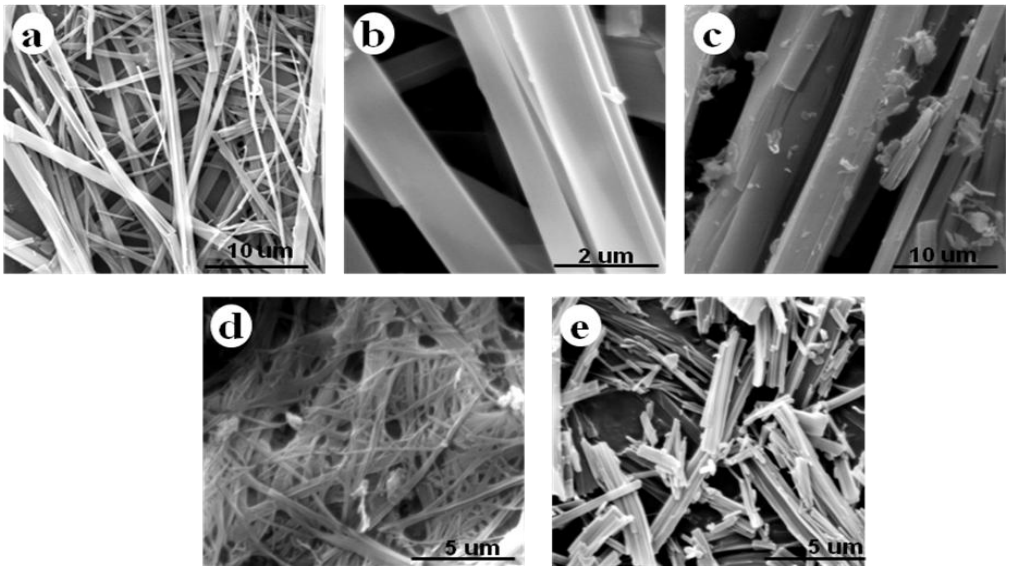

Figure S5: SEM images of of **2** in (a) toluene gel, (b) benzene gel, (c) cyclohexane, and SEM images of **3** in (d) toluene gel, (e) p-xylene gel at their CGCs.

11. XRD Studies:

The XRD patterns of the solid powdered compound and xerogel of toluene were collected by a Rigalcu D/Max-3c diffractometer with Cu Kα radiation (λ= 0.154 nm). The tube voltage and amperage were set at 40 kV and 30 mA respectively. Each sample was scanned between 1.6 º and 30 º(2θ) with a step size of 0.02º and the scan rate was 1°/min. Xerogels were made by drying the gels under vacuum for few hours at room temperature.

In order to obtain the information about molecular packing, XRD measurements of compound **2** and **3** were performed in both solid and gel state and the results are shown in Figure S6. As shown in that figure, the XRD pattern for **2** and **3** in both powder and gel state were found to be almost similar and this demonstrates that in both states each compound has similar molecular packing arrangement. The XRD spectrum of the xerogel of **2** from toluene (0.7 %, w/v) exhibited four major reflection peaks in the small angle region (2 theta = 5 to 15 degree) and the corresponding *d* spacings (1.47 nm, 1.04 nm, 0.73 nm and 0.66 nm) follow the ratio of about 1：1/√2：1/2: 1/√5. In this case, a tetragonal packing arrangement can be proposed with a basic distance 1.47 nm and that distance is closely related to the fully stretched molecular length of gelator **2** calculated from molecular dynamics simulation. In case of xerogel of **3,** reflection peaks d values ((2 theta = 5 to 12 degree) were found at 2.58 nm, 1.85 nm, 1.31 nm, 1.12 nm and 0.99 nm,0.93 and 0.89 respectively, corresponding to the ratio 1 : (1/√2): (1/2) : (1/√5) : (1/√7) : (1/√8) : (1/3) and the findings indicate the probable tetragonal packing mode in the self-assembly of compound **3** in gel state with a basic distance of 2.58 nm, which is close to the calculated molecular length of the dimer.

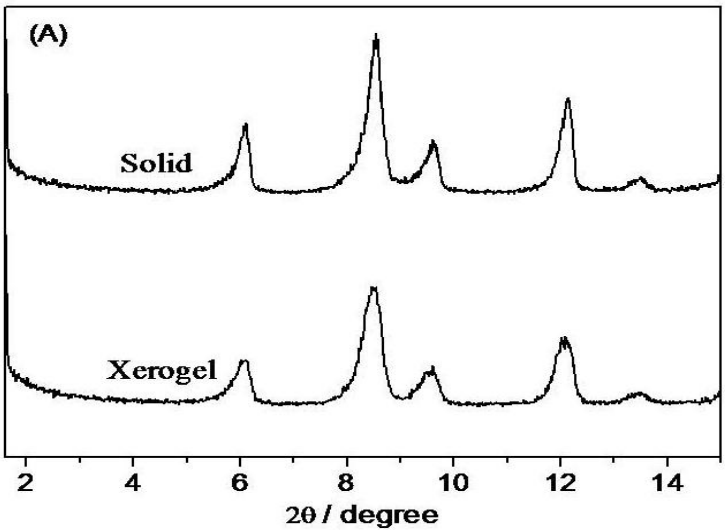

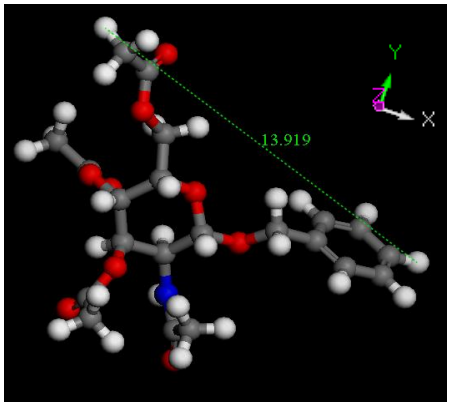

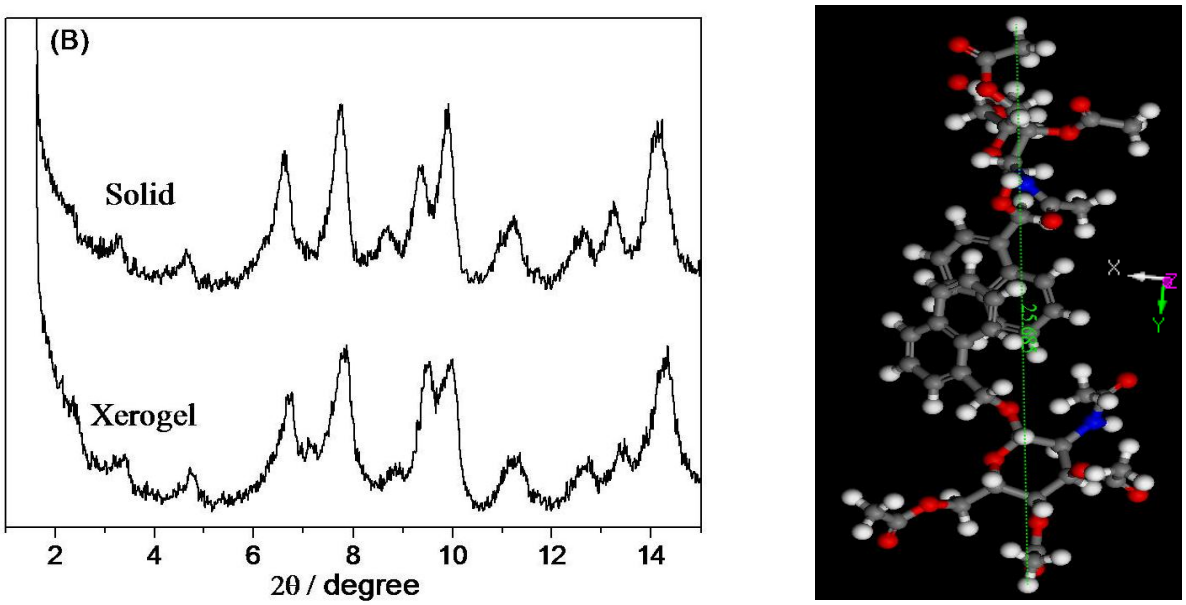

Figure S6. (A) XRD pattern of **2** in solid state and xerogel state from toluene at cgc. (B) XRD pattern of **3** in solid state and xerogel state from toluene at cgc.

12. Phase-selective gelation:

(A) Selective gelation of petrol by gelator 3: A required amount solution of **3** (12 mg in 0.1 mL THF) was added to the petrol/water mixture (0.8: 2) in a glass vial and within 15 s petrol layer was completely gelled selectively from its aqueous mixture. Within 50 s the petrol gel was strong enough and was stable to inversion with its own weight and weight of water on top. To recover both the petrol and gelator, petrol gel was heated to 56 ℃ (above T_{gel}) in the vacuum distillation process.

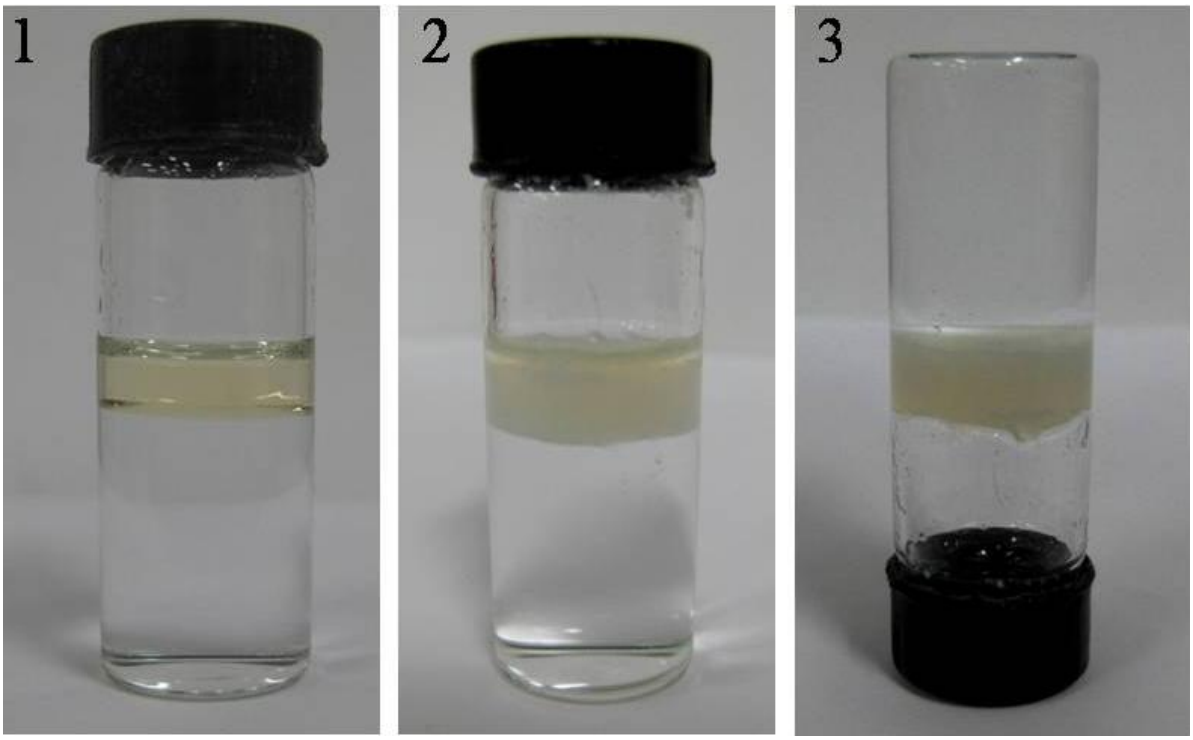

Figure S7: Selective gelation of petrol layer by **3** in a biphasic mixture of petrol and water at room temperature: (1) mixture of 2 mL water and 0.8 mL petrol, (2) complete selective gelation of petrol after addition of the solution of **3** within 15 s, and (3) within 50 s this petrol gel becomes stable to inversion of vial.

(B) Phase-selective gelation at low temperature: On the other hand, the temperature of the oil/water system is also an important matter for consideration in context of real scenario of oil spills. Hence, selective gelation should also be checked at temperatures lower than room temperature to increase the robustness of the model solidifier system. In this study, we have performed similar type of selective gelation experiment of diesel and petrol at low temperature. In a typical experiment, 2 mL water and 0.8 mL diesel were mixed together in a glass vial and that was placed in an ice bath where temperature of the water in the mixture can attain about 0-5 ℃ value. Then solution of the gelator (16 mg **2** in 0.1 mL THF) was added to that oil/water mixture and instantly the diesel phase was converted to a gel and within 45 s it was able to bear its own weight in an inverted vial. Thus, selective gelation time and efficiency were

found same as room temperature phase-selective gelation study. In addition, after selective gelation solidified oils were stable enough same as room temperature method.

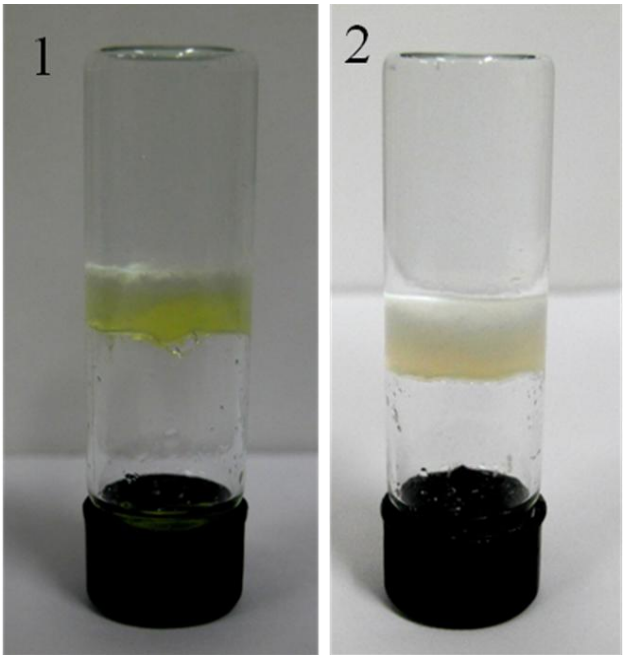

Figure S8: (1) photograph of the diesel gel of **2** in inverted vial after the selective gelation experiment in an ice bath, (2) photograph of the petrol gel of **3** in inverted vial after the selective gelation experiment in an ice bath. The temperature of the water was about 0-5 ℃ during these studies.

(C) Selective gelation of diesel layer by gelator 2 in a petri dish:

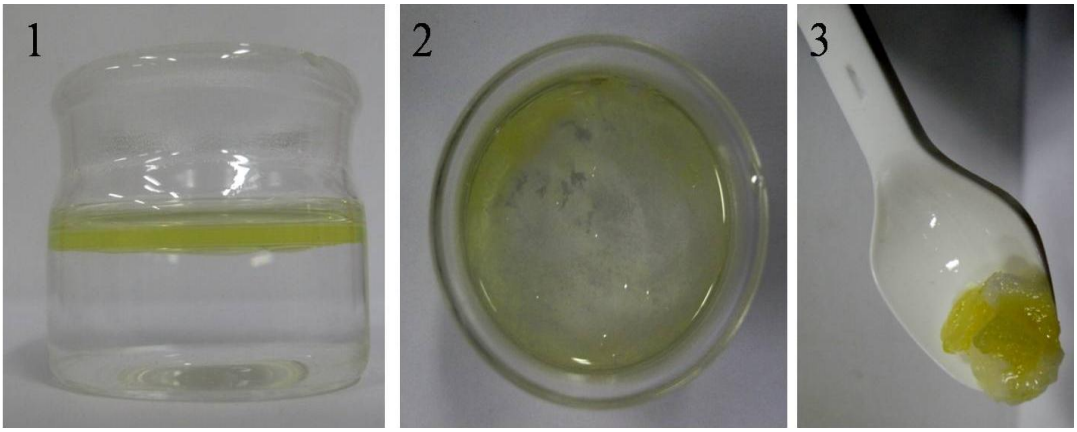

Figure S9: (1) thin layer of diesel floating on large volume of water (in a Petri dish), (2) instantaneous (within 20 s) selective gelation of diesel layer after addition of the solution of the gelator **2**, (3) diesel gel scooped out with a spatula.

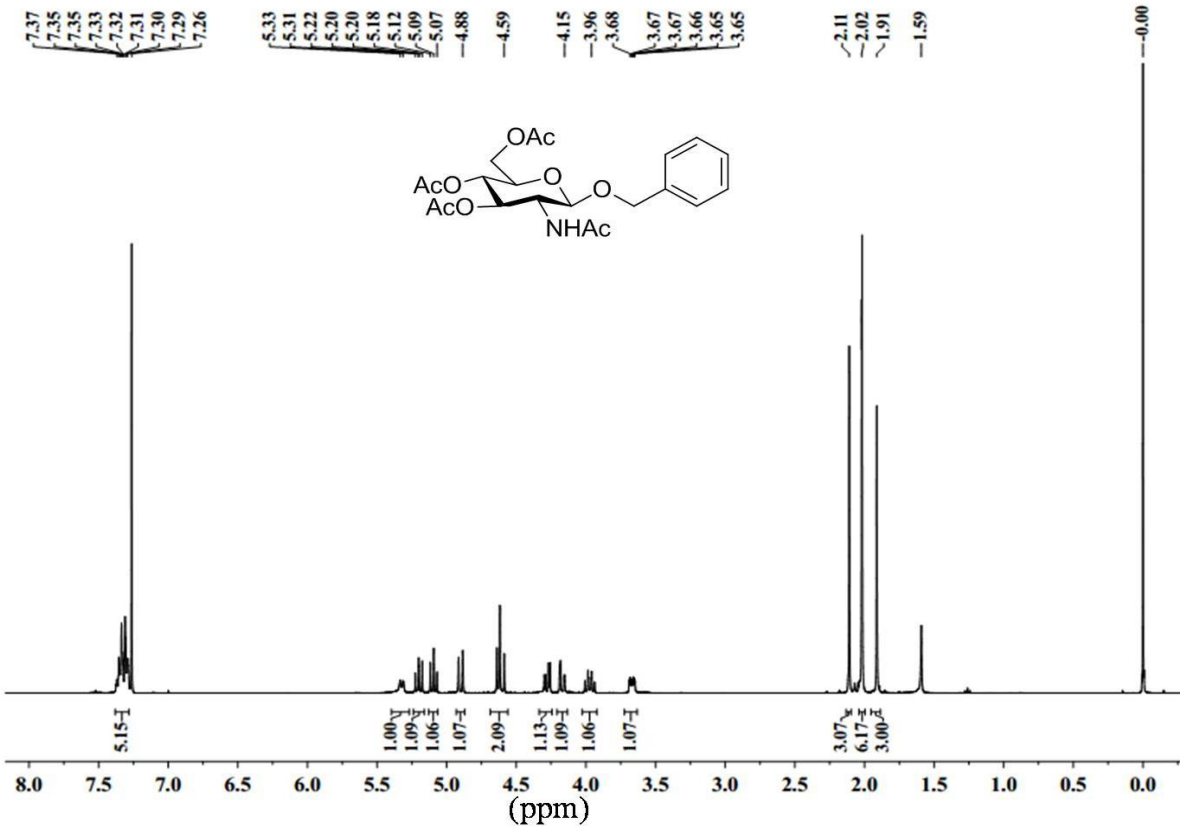
7.37
7.35
7.35
7.33
7.32
7.31
7.30
7.29
7.26
5.33
5.31
5.22
5.20
5.20
5.18
5.12
5.09
5.07
4.88
4.59
4.15
3.96
3.68
3.67
3.67
3.66
3.65
3.65
2.11
2.02
1.91
1.59
0.00
OAc
AcO
AcO
O
O
NHAc
5.15
1.00
1.09
1.06
1.07
2.09
1.13
1.09
1.06
1.07
3.07
6.17
3.00
8.0
7.5
7.0
6.5
6.0
5.5
5.0
4.5
4.0
3.5
3.0
2.5
2.0
1.5
1.0
0.5
0.0
(ppm)

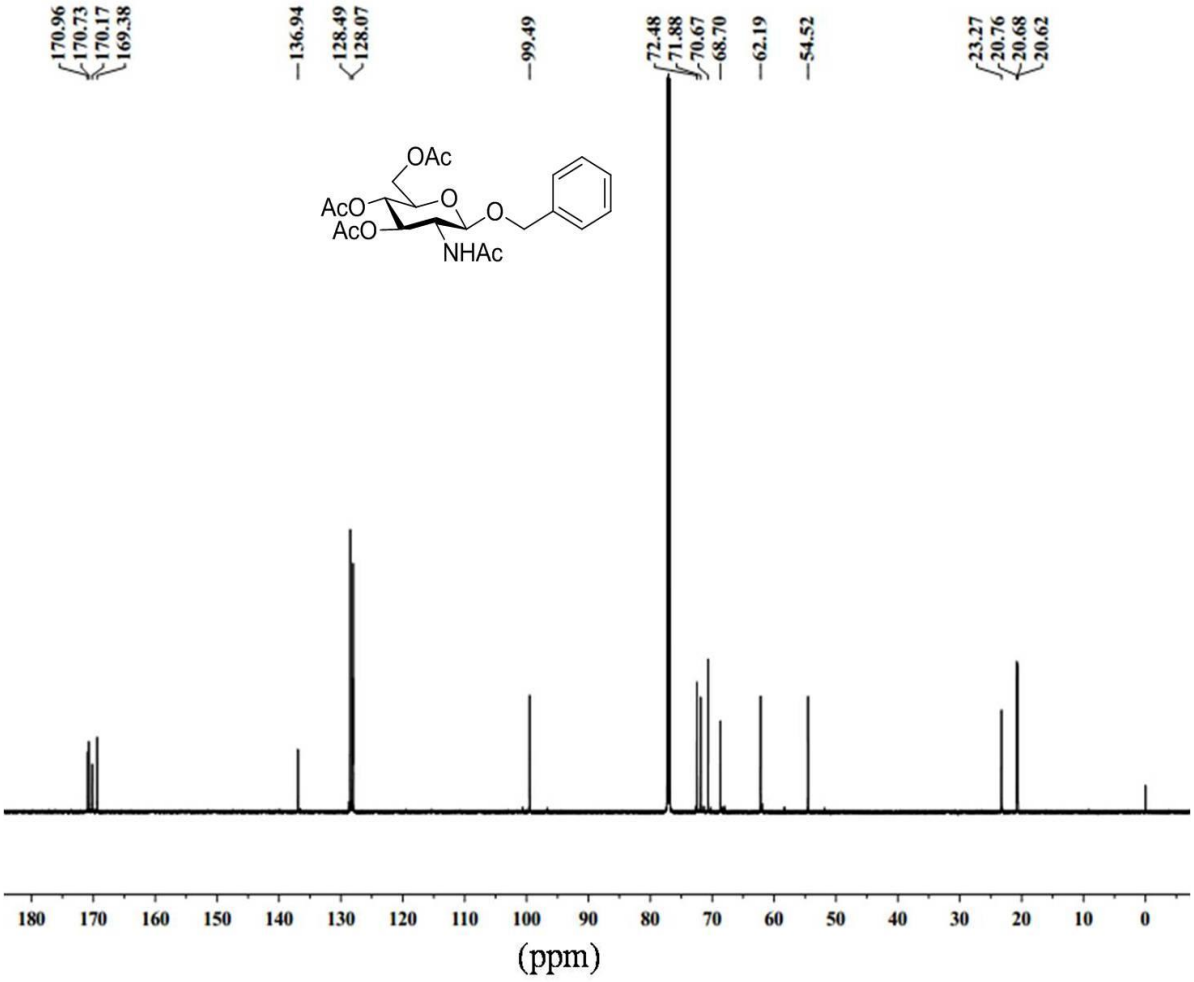
170.96
170.73
170.17
169.38
136.94
128.49
128.07
99.49
72.48
71.88
70.67
68.70
62.19
54.52
23.27
20.76
20.68
20.62
OAc
AcO
AcO
O
O
NHAc
180
170
160
150
140
130
120
110
100
90
80
70
60
50
40
30
20
10
0
(ppm)

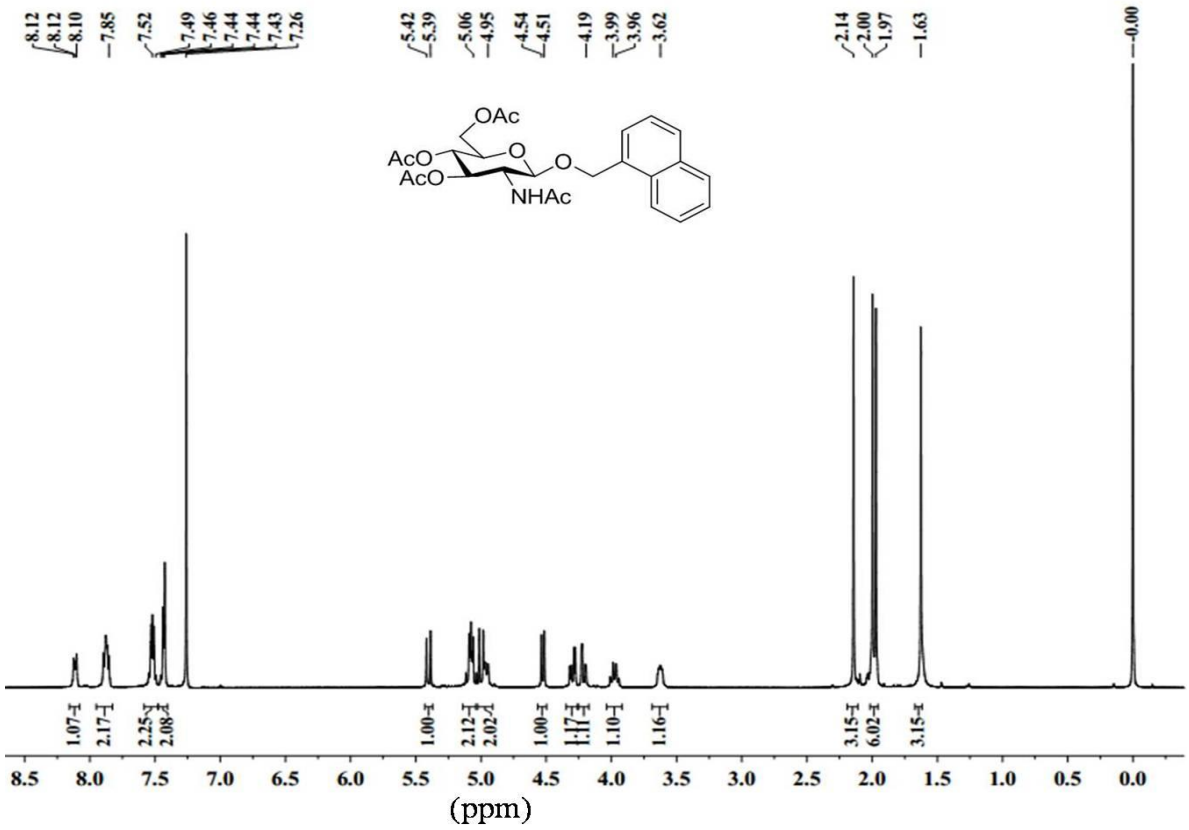
8.12
8.12
8.10
7.85
7.52
7.49
7.46
7.44
7.44
7.43
7.26
5.42
5.39
5.06
4.95
4.54
4.51
4.19
3.99
3.96
3.62
2.14
2.00
1.97
1.63
0.00
OAc
AcO
AcO
O
O
NHAc
1.07
2.17
2.25
2.08
1.00
2.12
2.02
1.00
1.17
1.11
1.10
1.16
3.15
6.02
3.15
8.5
8.0
7.5
7.0
6.5
6.0
5.5
5.0
4.5
4.0
3.5
3.0
2.5
2.0
1.5
1.0
0.5
0.0
(ppm)

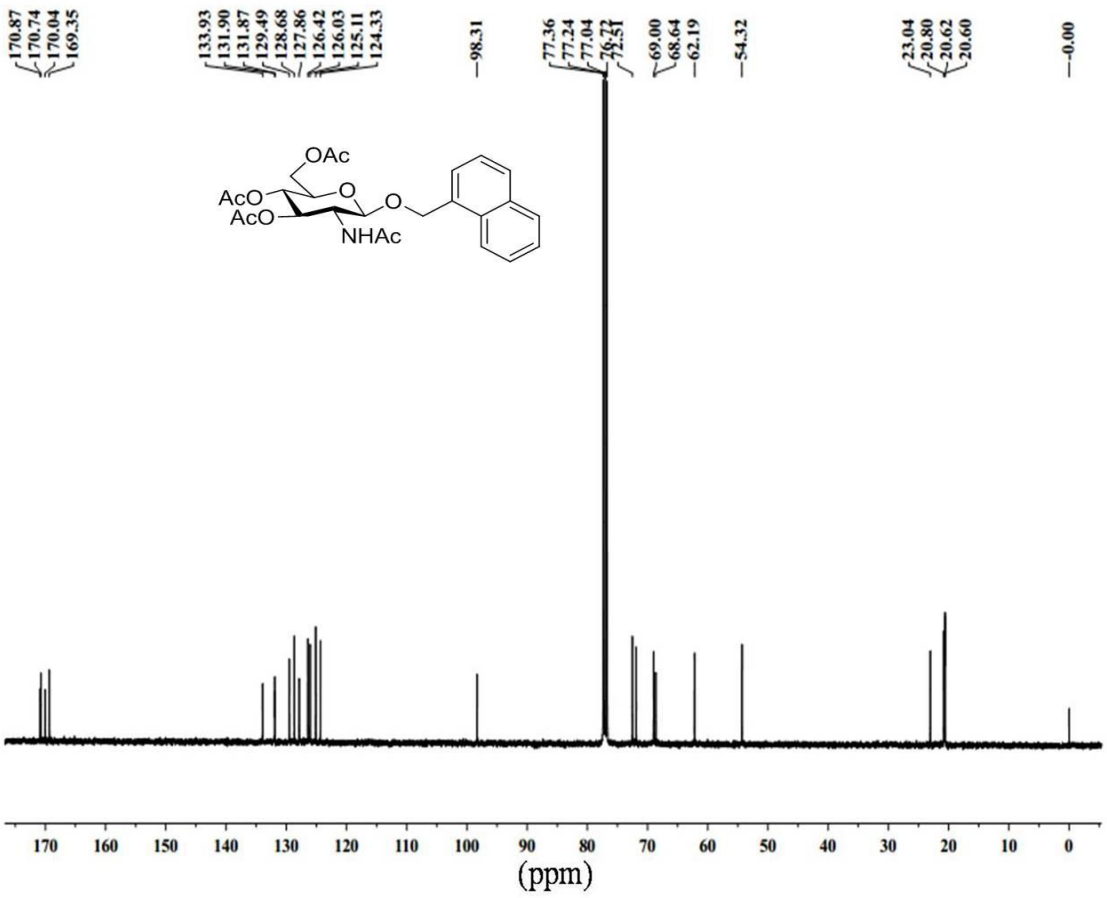
170.87
170.74
170.04
169.35
133.93
131.90
131.87
129.49
128.68
127.86
126.42
126.03
125.11
124.33
98.31
77.36
77.24
77.04
72.51
69.00
68.64
62.19
54.32
23.04
20.80
20.62
20.60
0.00
OAc
AcO
AcO
O
O
NHAc
170 160 150 140 130 120 110 100 90 80 70 60 50 40 30 20 10 0
(ppm)

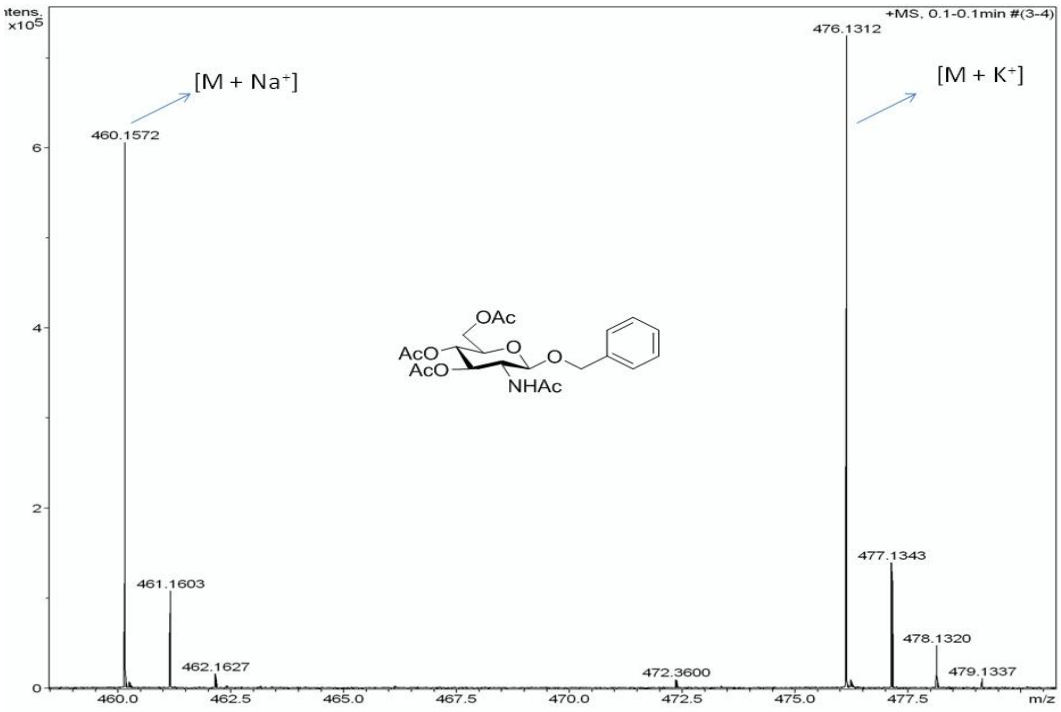
+MS, 0.1-0.1min #(3-4)
476.1312
[M + Na+]
[M + K+]
460.1572
OAc
AcO
AcO
O
O
NHAc
461.1603
462.1627
472.3600
477.1343
478.1320
479.1337
460.0
462.5
465.0
467.5
470.0
472.5
475.0
477.5
m/z

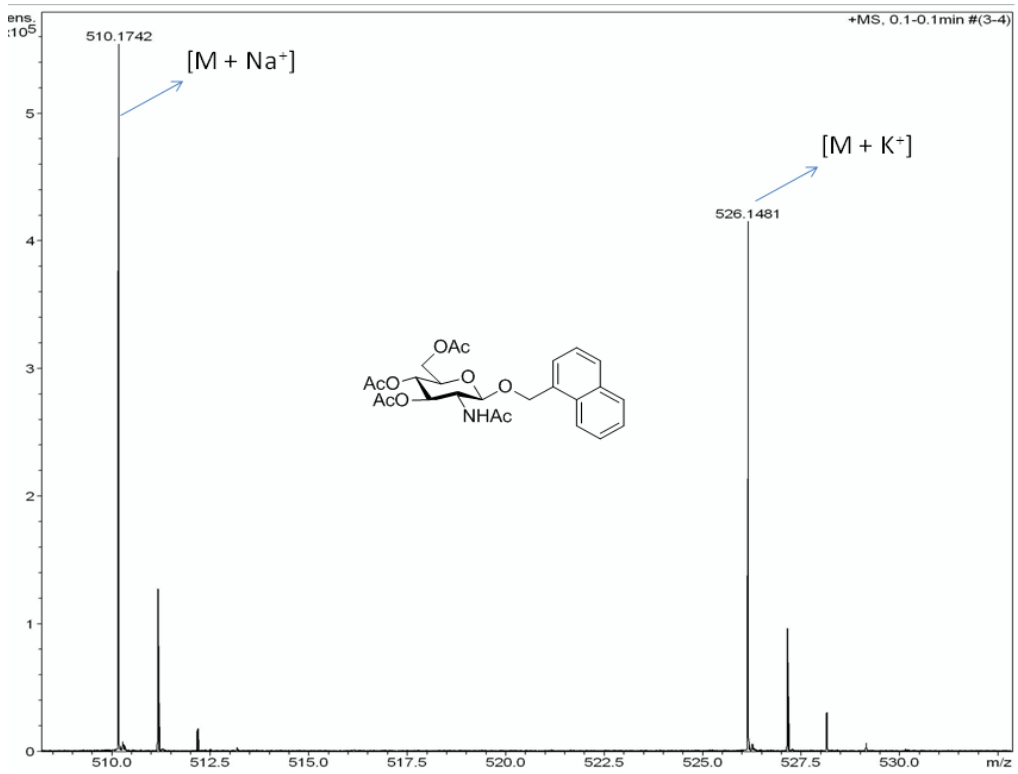
+MS, 0.1-0.1min #(3-4)
510.1742
[M + Na+]
[M + K+]
526.1481
OAc
AcO
AcO
O
O
NHAc
510.0
512.5
515.0
517.5
520.0
522.5
525.0
527.5
530.0
m/z

References:

1. B. Aguilera, A. Fernandez-Mayoralas and C. Jaramillo, *Tetrahedron*, 1997, **53**, 5863–5876.

2. (a) B. Escuder, S. Martl and J. F. Miravet, *Langmuir*, 2005, **21**, 6776-6787; (b) J. H. Jung, S. Shinkai and T. Shimizu, *Chem. Eur. J*., 2002, **8**, 2684-2690; (c) M. Hashimoto, S. Ujiie and A. Mori, *Adv. Mater*., 2003, **15**, 797-800.